Journal of King Saud University – Science 35 (2023) 102618

HOSTED BY

Contents lists available at ScienceDirect

Journal of King Saud University – Science

journal homepage: www.sciencedirect.com

Original article

Analysis and numerical simulation of fractal-fractional order non-linear couple stress nanofluid with cadmium telluride nanoparticles

Saqib Murtaza [a], Zubair Ahmad [b], Ibn E. Ali [c], Z. Akhtar [d], Fairouz Tchier [e], Hijaz Ahmad [f,g], Shao-Wen Yao [h,*]

[a] Department of Mathematics, Faculty of Science, King Mongkut's University of Technology Thonburi (KMUTT), 126 Pracha Uthit Rd., Bang Mod, Thung Khru, Bangkok 10140, Thailand
[b] Department of Mathematics and Physics, University of Campania "Luigi Vanvitelli", Caserta 81100, Italy
[c] Higher Education Archives & Libraries Department KP, Govt. Superior Science College, Peshawar, Pakistan
[d] Division of Science and Technology, University of Education, Township, Lahore 54590, Pakistan
[e] Department of Mathematics, College of Science, King Saud University, P.O. Box 2455, Riyadh 11451, Saudi Arabia
[f] Near East University, Operational Research Center in Healthcare, Near East Boulevard, PC: 99138 Nicosia/Mersin 10, Turkey
[g] Section of Mathematics, International Telematic University Uninettuno, Corso Vittorio Emanuele II, 39, 00186 Roma, Italy
[h] School of Mathematics and Information Science, Henan Polytechnic University, Jiaozuo 454000, China

ARTICLE INFO

Article history:
Received 23 April 2022
Revised 15 February 2023
Accepted 18 February 2023
Available online 25 February 2023

Keywords:
Fractal-fractional derivative
Couple stress fluid
Cadmium telluride nanoparticles
Mineral transformer oil
Crank-Nicolson scheme

ABSTRACT

It is generally considered that fractal-fractional order derivative operators are highly sophisticated mathematical tools that can be applied in a variety of physics and engineering situations to obtain real solutions. By using fractal-fractional derivatives, we can simultaneously investigate fractional order and fractal dimension. Due to extensive applications of fractal-fractional derivatives, in the present article fractal-fractional order model of non-linear Couple stress nanofluid has been analyzed. The homogenous mixture of base fluid and nanoparticles has been formed by the uniform dispersion of cadmium telluride nanoparticles in mineral transformer oil. Primarily, the classical mathematical model has been formulated via relative constitutive equations and then generalized by using fractal-fractional derivative operator. This model has been numerically solved using Crank-Nicolson technique. Using numerical solutions, various graphs are plotted to analyze how physical parameters alter Couple stress nanofluid rheology. As can be seen from the graphical study, couple stress slows down fluid velocity. Adding cadmium telluride nanoparticles to transformer oil increased its efficacy by 15.27%.

1. Introduction

A nanofluid can simply be defined as a mixture of two-phase solid particles dispersed in a fluid, such as water, air, oils, etc., within nanoscales. It has been apparent for a long time that the scientific community has been trying to improve the qualities of various liquids, and they have also been trying to correct the insufficiencies of these liquids. A millimeter sized metallic particle and a micron sized metallic particle were used in this study by researchers and analysts. To improve thermal conductivity, Maxwell proposed spreading metallic particles in normal base fluids (Maxwell James C., 1873). Clogging, channel erosion, and sedimentation are among issues that it faces. By introducing micro-sized solid particles to the base fluids, Masuda et al. studied the heat transfer rate of the fluids and their thermal properties, but they ran into the same problems as Maxwell's theory in their studies (Masuda et al., 1993). Later on, Hamilton-Crosses (Hamilton and Crosser, 1962) extended Maxwell's work and came up with a more accurate solution based on Maxwell's idea. The first time nano-sized particles were used in base liquids was done by Choi (Choi and Eastman, 1995) in 1995, and he was the first experimentalist to do so. It is recommended that the volume fraction is restricted to a range ranging from 0.0 to 0.04 in order to avoid the formation of sedimentation and clogging problems that can arise if we increase the number of nanoparticles.The use of nanoparticles in base liquids has been identified to boost thermal conduction and heat transfer rates, according to many studies. There will be a disturbance in the flow of fluid as a result of this. In addition to enhancing the properties of conventional liquids, these additives are also able to enhance their thickness, lubricity, breakdown voltage, and dielectric strength. The thermal conduction of such liquids and the rate of heat transfer within them are quite limited. By disbanding graphene and molybdenum disulfide in the base liquid, Arif *et al.* investigated the heat transmission rate (Arif et al., 2019). Khan *et al.* examined at the homogeneous and

* Corresponding author.
E-mail address: yaoshaowen@hpu.edu.cn (S.-W. Yao).

https://doi.org/10.1016/j.jksus.2023.102618
1018-3647/

Nomenclature

Symbol	Name
μ	Dynamic Viscosity
β_T	Thermal Expansion Coefficient
D	Mass Diffusion Rate
$\vec{J}$	Current Density
G	External Pressure Gradient
Gm	Mass Grashof Number
Ec	Eckert Number
Re	Reynold Number
α	Fractional Order
h	Space Length
IBCS	Initial and Boundary Conditions
ρC_p	Specific Heat Capacity
β_C	Concentrtation coefficient
k	Thermal Conductivity
$\vec{B}$	Induced Magnetic Field
η	Couple Stress Parameter
Gr	Thermal Grashof Number
Pr	Prandtl Number
Sc	Schmidth Number
β	Fractal Dimension
λ	Time Length
M, N	Number of Grid Points

heterogeneous chemical processes that happen in nanofluid as it moves through a channel. The authors also considered the effects of bioconvection in their research (Khan and Puneeth, 2021). Rasheed *et al.* (Rasheed et al., 2021) studied nanofluid MHD flow in the presence of Newtonian heating, advection energy, and convective conditions. The stationary magnetic field was also taken into account by the researchers. Shahzad *et al.* examined Jeffrey nanofluid flow driven to Lorentz force and viscous dissipation. They found in their study that Graphene-based nanofluid has greater temperature than regular fluid (Shahzad et al., 2021). few important and significant studies on nanofluid's application can be found in (Hasin et al., 2022; Murtaza et al., 2020).

The traditional Navier-Stokes principle cannot capture the exact behavior of some liquids, such as polymeric liquids, colloidal suspensions, liquids containing added substances, and liquids composed of arbitrarily positioned particles. Analysts presented numerous models to investigate the properties of these fluids. Stokes' (Stokes and Stokes, 1984) developed the couple stress theory for liquids that differ from traditional Newtonian viscous liquids in a number of ways. Couple stress theory, which includes couple stress, antisymmetric stress tensor, and body couples, is more broad than Newtonian viscous fluid theory. These kinds of fluids contain haphazardly arranged and unbending particles. Couple stresses' major objective is to define the size impact of these liquids, which cannot be adequately represented by Newton's fluid theory. CSF is a viscous liquid containing irregularly shaped and stiff particles such as liquid crystals, lubricants, blood, and other materialsIt is characterised as a couple stress tensor when the spin field upshots in an antisymmetric stress tensor are due to the rotation of free moving particles in an antisymmetric stress tensor. This points us to the idea of couple stresses. By studying these fluids, it is possible to explain the behavior of numerous polymer suspensions, lubricants, liquid crystals, and other materials. Because of these properties, other researchers have used CSF to investigate the characteristics of various fluids. As an example, Srivastava examined the behaviour of blood flow passing through a stenotic blood vessel by considering blood to be a fluid in a couple of stresses (Biomechanics and 1985, n.d.). After increasing the couple stress parameters, he discovered that there was an increase in resistance to blood flow and wall shear stress when he increased the couple stress parametersA comparison has also been made between the results of the experiment and the Newtonian fluid model. There is a finding that the wall shear stress and blood flow are higher for the couple stress fluid model than for the single stress fluid model. A penetrating catheter filled with microscopic gold particles was used to study blood flow as CSF via blocked arteries of the heart (Ellahi et al., 2019). They discovered that gold particles enclose big molecules that deliver medications to the organ's damaged area. Couple-stresses have an impact on lubrication challenges when additives are applied or if the lubricant comprises long-chain molecules. Couple-stresses of this nature have the potential to have a major influence on bearing behaviour in practise. Lin examined the CSF properties of lubricated journal bearings owing to the lubricant combined with various additives (International and 1998, n.d.). According to him, CSF boosts the load-carrying capacity and improves the journal-bearing properties of bearings as well as producing more apparent effects than Newtonian lubricants in terms of their benefits to bearings. In a recent study, Naduvinamani et al. (Naduvinamani and Kashinath, 2006) investigated the interaction between rough surfaces and the lubrication of a porous journal bearing using CSF to serve as the lubricant. During their study, they discovered that roughness in a fluid has a greater impact on its bearing properties than smoothness in a Newtonian fluidSeveral stress fluid models of blood flow through a stenosed tube have been developed (Pralhad and Schultz, 2004). A few further applications were discussed as well, such as polycythemia, plasma cell dichasia, and sickle cell disease, where their study was applied. By increasing the stress parameters of a porous channel within a microcirculatory system, Tripathi (Tripathi, 2011) observed that pressure was reduced by reducing peristaltic blood flow as CSFF through a porous channel. CSF flow is also being used in modern technologies and modern medicine for a number of additional purposes, including biomedicine (Ramesh et al., n.d.), digestive issues (Shit et al., n.d.), gland tumors, and arthritis (Hussain et al., n.d.).

The mathematics of fractional calculus involves derivatives and integrals with arbitrary orders.The concept of fractional calculus extends the classical notion of derivatives and integrals to non-integer orders, which allows for the modeling of complex phenomena and processes with memory and hereditary effects. This field has applications in a wide range of areas, including physics, engineering, finance, and biology (Ahmad et al., 2021; Almalahi et al., 2021b, 2021c, 2021a; Atangana, 2017; Atangana and İğret Araz, 2020; Atangana and Qureshi, 2019). Fractional calculus has several important applications in various fields such as physics, engineering, finance, and biology. Some of the significant uses and practical applications of fractional calculus are: Fractional calculus allows for the modeling of complex systems, such as viscoelastic materials, electrical circuits, and fluid flow, that exhibit memory and non-local behavior. Fractional calculus has been used in control and optimization theory, particularly in fractional order PID controllers and fractional optimization algorithms. Fractional calculus has been used in the design of fractional-order filters for signal processing, which can provide improved performance over traditional integer-order filters in some applications. Fractional calculus has been applied in financial mathematics, where it has been used to model the behavior of stock prices, interest rates, and other financial instruments. Fractional calculus has also been used to

model biological processes, such as the spread of diseases, blood flow, and the mechanics of biological tissues. These are some of the most significant applications of fractional calculus, but there are many more areas where it is used to provide more accurate and comprehensive models (Abro and Atangana, 2020; Heydari, 2020; Murtaza et al., 2022a).

According to the author, the literature on the flow of couple-stress fluid through an open channel is very rare, and none has addressed the flow of couple-stress nanofluid (CSNF) with viscous dissipation and time-dependent boundary conditions. It is because of this reason that the present study determines the effect of mass and heat transfer, viscous diffusion, and time-dependent boundary conditions on CSNF flow. The problem is modelled in terms of highly non-linear integer order coupled PDEs which is then transformed to the fractal-fractional model by incorporating time derivative with time fractal-fractional derivative. Due to the difficulty of solving such non-linear problems, Crank-Nicolson technique are used through Mathematica. The graphical and numerical results are portrayed through different graphs and tables and discussed in detail.

2. Formulation of mathematical model

Using a microchannel of length l, we studied nonlinear fractal-fractional Couple stress nanofluid. We have also taken into account the effect of viscous dissipation and the external pressure gradient as part of our analysis. The initial assumption is that fluid and plates will remain static at ambient temperature and concentration for a fixed period of time. The left plate of the fluid is disturbed by a velocity of magnitude $U_0H(\tau)$ at the time $\tau > 0$, and this motion is transmitted by the fluid to the right plate When t becomes greater than 0, the temperature of the fluid as well as the concentration of the fluid rises to $T_s + (T_p - T_s)A\tau$ and $C_s + (C_p - C_s)A\tau$ respectively. Fig. 1 illustrates the geometric representation of the problem in more detail.

For nanofluid model the governing equations are given as (Akhtar and Shah, 2018; Ali et al., 2020):

$$\rho_{nf}\frac{\partial v(y,\tau)}{\partial \tau} = G^* + \mu_{nf}\frac{\partial^2 v(y,\tau)}{\partial y^2} - \eta\frac{\partial^4 v(y,\tau)}{\partial y^4} + g(\rho\beta_T)_{nf}(T(y,\tau) - T_s) + g(\rho\beta_C)_{nf}(C(y,\tau) - C_s), \tag{1}$$

$$(\rho c_p)_{nf}\frac{\partial T(y,\tau)}{\partial \tau} = k_{nf}\frac{\partial^2 T(y,\tau)}{\partial y^2} + \mu_{nf}\left(\frac{\partial v}{\partial y}\right)^2, \tag{2}$$

$$\frac{\partial C(y,\tau)}{\partial \tau} = D_{nf}\frac{\partial^2 C(y,\tau)}{\partial y^2}, \tag{3}$$

IBCs are:

$$\left.\begin{array}{lll} v(y,0) = 0, & T(y,0) = T_s, & C(y,0) = C_s, \\ v(0,\tau) = 0, & T(0,\tau) = T_s, & C(0,\tau) = C_s, \\ v(l,\tau) = U_0H(\tau), & T(l,\tau) = T_s + (T_p - T_s)A\tau, & C(l,\tau) = C_s + (C_p - C_s)A\tau. \end{array}\right\} \tag{4}$$

The thermophysical properties of the considered base fluid and nanoparticles are given in Table 1 while the nanofluid correlations are given as (Ali et al., 2020; Murtaza et al., 2020).

$$\mu_{nf} = \mu_{TO}(1-\varphi_{CT})^{-2.5}, \quad D_{nf} = D_{TO}(1-\varphi_{CT}),$$
$$\rho_{nf} = (1-\varphi_{CT})\rho_{TO} + \varphi_{CT}\rho_{CT},$$
$$(\rho\beta_T)_{nf} = (\rho\beta_T)_{TO}(1-\varphi_{CT}) + \varphi_{CT}(\rho\beta_T)_{CT},$$
$$(\rho\beta_C)_{nf} = (\rho\beta_C)_{TO}(1-\varphi_{CT}) + \varphi_{CT}(\rho\beta_C)_{CT},$$
$$(\rho C_p)_{nf} = (1-\varphi_{CT})(\rho C_p)_{TO} + \varphi_{CT}(\rho C_p)_{CT},$$
$$\sigma_{nf} = \sigma_{TO}\left[1 + \frac{3\left(\frac{\sigma_{CT}}{\sigma_{TO}} - 1\right)\varphi_{CT}}{\left(\frac{\sigma_{CT}}{\sigma_{TO}} + 2\right) - \left(\frac{\sigma_{CT}}{\sigma_{TO}} - 1\right)\varphi_{CT}}\right],$$
$$k_{nf} = k_{TO}\left[\frac{k_{CT} + 2k_{TO} - 2\varphi_{CT}(k_{TO} - k_{CT})}{k_{CT} + 2k_{TO} + \varphi_{CT}(k_{TO} - k_{CT})}\right].$$

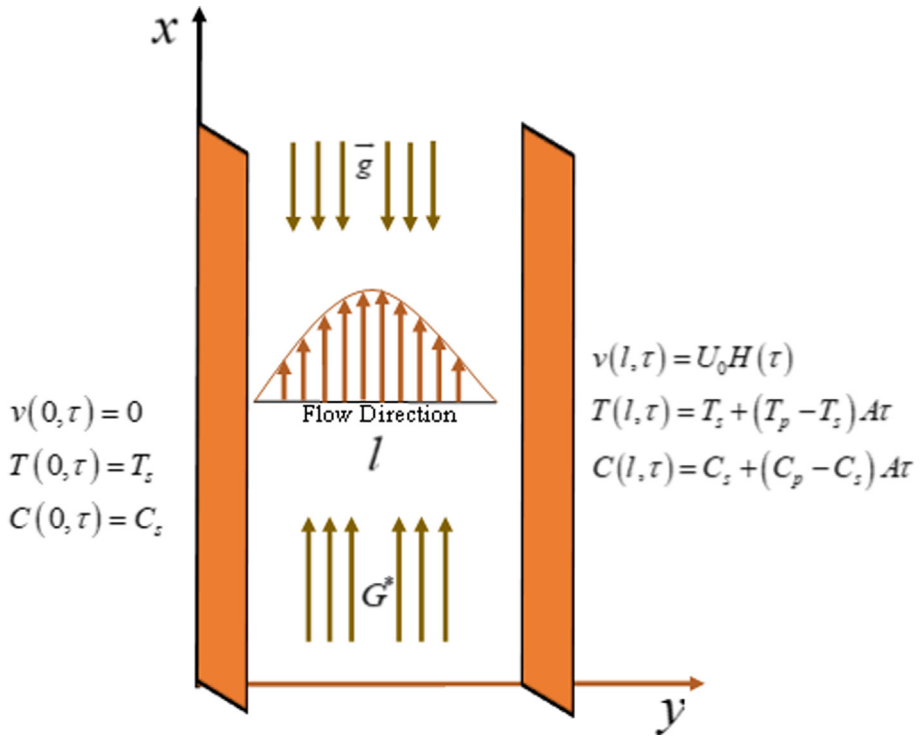

Fig. 1. Geomertical Illusration of the Model.

Table 1
Cadmium Telluride Nanoparticles and Transformer Oil: Thermomechanical Characteristic (Ghaffarkhah et al., 2020; Murtaza et al., 2022b).

	$\rho(kg/m^3)$	$C_p(J/kgK)$	$K(W/mK)$	$\beta_T \times 10^{-5}\left(K^{-1}\right)$	$\sigma(Sm^{-1})$
Cadmium Telluride	5855	209	7.5	0.00005	0.0000007
Transformer Oil	861	1860	0.157	0.75	1.57×10^{-8}

Following are the dimensionless variables:

$$\left.\begin{aligned} &\zeta = \tfrac{y}{\ell},\ u = \tfrac{u}{U_0},\ t = \tfrac{U_0\tau}{\ell},\ \aleph = \tfrac{\eta}{\mu_f \ell^2},\\ &G = \tfrac{\ell^2}{\mu_f U_0} G^*,\ \Theta = \tfrac{T-T_s}{T_p-T_s},\ \Phi = \tfrac{C-C_s}{C_p-C_s}. \end{aligned}\right\} \tag{5}$$

Using these dinmensionless entities, the govering equations will be;

$$\frac{\partial u(\zeta,t)}{\partial t} = G + \Re_1 \frac{\partial^2 u(\zeta,t)}{\partial \zeta^2} - \eta \frac{\partial^4 u(\zeta,t)}{\partial \zeta^4} + Gr\Theta(\zeta,t) + Gm\Phi(\zeta,t), \tag{6}$$

$$\frac{\partial \Theta(\zeta,t)}{\partial t} = \frac{1}{\hbar_2} \frac{\partial^2 \Theta(\zeta,t)}{\partial \zeta^2} + \psi \left(\frac{\partial u(\zeta,t)}{\partial \zeta}\right)^2, \tag{7}$$

$$\frac{\partial \Phi(\zeta,t)}{\partial t} = \Im \frac{\partial^2 \Phi(\zeta,t)}{\partial \zeta^2}, \tag{8}$$

and

$$\left.\begin{aligned} &u(\zeta,0) = 0, \quad \Theta(\zeta,0) = 0, \quad \Phi(\zeta,0) = 0,\\ &u(0,t) = 0, \quad \Theta(0,t) = 0, \quad \Phi(0,t) = 0,\\ &u(1,t) = 1, \quad \Theta(1,t) = t, \quad \Phi(1,t) = t, \end{aligned}\right\} \tag{9}$$

here

$$\begin{aligned} &G = \tfrac{G^* \mu_{TO} U_0}{\ell^3 \rho_{TO} n_1},\ \Re_1 = \tfrac{\mu_{TO} n_2 U_0}{\ell^3 \rho_{TO} n_1},\ \eta = \tfrac{\chi \mu_{TO} U_0}{\ell^3 \rho_{TO} n_1},\ Gr = \tfrac{(\rho\beta_T)_{TO} n_3 (T_p - T_s)}{\ell \rho_{TO} n_1},\\ &Gm = \tfrac{(\rho\beta_C)_{TO} n_4 (C_p - C_s)}{\ell \rho_{TO} n_1}, \Pr = \tfrac{(\mu C_p)_{TO}}{K_{TO}},\ E_c = \tfrac{v_{TO} U_0}{(C_p)_{TO}(T_p - T_s)\ell},\\ &Re = \tfrac{U_0 \ell}{\upsilon},\ \hbar_2 = \tfrac{\Pr Rem_1}{m_2},\ \psi = \tfrac{E_c n_2}{m_1},\ Sc = \tfrac{v_{TO}}{D_{TO}},\ \Im = \tfrac{(1-\varphi)}{ScRe},\\ &n_1 = (1-\varphi) + \tfrac{\varphi \rho_{CT}}{\rho_{TO}},\ n_2 = (1-\varphi)^{-2.5},\ n_3 = (1-\varphi) + \tfrac{\varphi(\rho\beta_T)_{CT}}{(\rho\beta_T)_{TO}},\\ &n_4 = (1-\varphi) + \tfrac{\varphi(\rho\beta_C)_{CT}}{(\rho\beta_C)_{TO}}, m_1 = (1-\varphi) + \tfrac{\varphi(\rho C_p)_{CT}}{(\rho C_p)_{TO}},\\ &m_2 = \frac{k_{CT} + 2k_{TO} - 2\varphi(k_{TO} - k_{CT})}{k_{CT} + 2k_{TO} + \varphi(k_{TO} - k_{CT})}. \end{aligned} \tag{10}$$

The classical model given in Eqs. (6)–(8) are transformed into fractal-fractional model by simply incorporating the time fractal-fractional derivative with ordinary time derivative and addressed as following:

$${}^{FF}D_t^{\alpha} u(\zeta,t) = \beta t^{\beta-1} \left\{ \begin{matrix} G + \Re_1 \frac{\partial^2 u(\zeta,t)}{\partial \zeta^2} - \eta \frac{\partial^4 u(\zeta,t)}{\partial \zeta^4} \\ + Gr\Theta(\zeta,t) + Gm\Phi(\zeta,t) \end{matrix} \right\} - \frac{u(\zeta,0)}{\Gamma(1-\alpha)} t^{-\alpha}, \tag{11}$$

$${}^{FF}D_t^{\alpha} \Theta(\zeta,t) = \beta t^{\beta-1} \left\{ \frac{1}{\hbar_2} \frac{\partial^2 \Theta(\zeta,t)}{\partial \zeta^2} + \psi \left(\frac{\partial u(\zeta,t)}{\partial \zeta}\right)^2 \right\} - \frac{\Theta(\zeta,0)}{\Gamma(1-\alpha)} t^{-\alpha}, \tag{12}$$

$${}^{FF}D_t^{\alpha} \Phi(\zeta,t) = \beta t^{\beta-1} \left\{ \Im \frac{\partial^2 \Phi(\zeta,t)}{\partial \zeta^2} \right\} - \frac{\Phi(\zeta,0)}{\Gamma(1-\alpha)} t^{-\alpha}. \tag{13}$$

Incorporating initial conditions in Eqs. (11)–(13), we get:

$${}^{FF}D_t^{\alpha} u(\zeta,t) = \beta t^{\beta-1} \left\{ \begin{matrix} G + \Re_1 \frac{\partial^2 u(\zeta,t)}{\partial \zeta^2} - \eta \frac{\partial^4 u(\zeta,t)}{\partial \zeta^4} \\ + Gr\Theta(\zeta,t) + Gm\Phi(\zeta,t) \end{matrix} \right\}, \tag{14}$$

$${}^{FF}D_t^{\alpha} \Theta(\zeta,t) = \beta t^{\beta-1} \left\{ \frac{1}{\hbar_2} \frac{\partial^2 \Theta(\zeta,t)}{\partial \zeta^2} + \psi \left(\frac{\partial u(\zeta,t)}{\partial \zeta}\right)^2 \right\}, \tag{15}$$

$${}^{FF}D_t^{\alpha} \Phi(\zeta,t) = \beta t^{\beta-1} \left\{ \Im \frac{\partial^2 \Phi(\zeta,t)}{\partial \zeta^2} \right\}. \tag{16}$$

Here ${}^{FF}D_t^{\alpha,\beta}$ is the fractal-fractional operator (Atangana, 2017) and expressed as:

$${}^{FF}D_t^{\alpha,\beta} \delta(t) = \frac{\Pi(\alpha)}{\Gamma(1-\alpha)} \frac{d}{dt^{\beta}} \int_0^t e^{-\frac{\alpha(t-\zeta)}{1-\alpha}} \delta(\zeta) d\zeta, \quad 0 < \alpha, \beta \le 1. \tag{17}$$

Eq. (17) follows the following property;

$$\Pi(0) = \Pi(1) = 1.$$

The finite difference technique can be used to discretize the first order fractal-fractional order derivative as:

$${}^{FF}\wp_{\tau}^{\alpha} \delta(\zeta,\tau) = \beta \tau^{\beta-1} \frac{\Pi(\alpha)}{2\alpha} \left\{ \frac{\delta_i^{j+1} - \delta_i^j}{\lambda} + \sum_{j=1}^{m} \left(\frac{\delta_i^{j+1-m} - \delta_i^{j-m}}{\lambda} + O(t) \right) \right\} \varpi_{j,m}, \tag{18}$$

$$\varpi_{j,m} = erf\left\{ \frac{\alpha j}{1-\alpha} (m-j) \right\} - erf\left\{ \frac{\alpha j}{1-\alpha} (m-j+1) \right\}.$$

Discretization through Crank-Nicolson method for second and fourth order derivative w.r.t space variable is given as follow:

$$\frac{\partial^2 \delta(\zeta,t)}{\partial \zeta^2} = \frac{1}{2h^2} \left\{ \left(\delta_{i+1}^{j+1} - 2\delta_i^{j+1} + \delta_{i-1}^{j+1} \right) + \left(\delta_{i+1}^{j} - 2\delta_i^{j} + \delta_{i-1}^{j} \right) \right\} + O(t), \tag{19}$$

$$\frac{\partial^4 \delta(\zeta,t)}{\partial \zeta^4} = \frac{1}{2h^4} \left\{ \begin{matrix} \left(\delta_{i+2}^{j+1} - 4\delta_{i+1}^{j+1} + 6\delta_i^{j+1} - 4\delta_{i-1}^{j+1} + \delta_{i-2}^{j+1} \right) \\ + \left(\delta_{i+2}^{j} - 4\delta_{i+1}^{j} + 6\delta_i^{j} - 4\delta_{i-1}^{j} + \delta_{i-2}^{j} \right) \end{matrix} \right\} + O(t), \tag{20}$$

with the above discretization given in Eqs. (19)–(20), the generalized governing Eqs. will take the shape:

$$\begin{aligned} &\frac{\Pi(\alpha)}{2\alpha} \left\{ \begin{matrix} \frac{u_i^{j+1} - u_i^j}{\lambda} \\ + \sum_{j=1}^{m} \left(\frac{u_i^{j+1-m} - u_i^{j-m}}{\lambda} \right) \end{matrix} \right\} \varpi_{j,m} \\ &= \beta t^{\beta-1} \left\{ \begin{matrix} G + \Re_1 \frac{1}{2h^2} \left(\begin{matrix} \left(u_{i+1}^{j+1} - 2u_i^{j+1} + u_{i-1}^{j+1} \right) \\ + \left(u_{i+1}^{j} - 2u_i^{j} + u_{i-1}^{j} \right) \end{matrix} \right) \\ \eta \frac{1}{2h^4} \left(\begin{matrix} \left(u_{i+2}^{j+1} - 4u_{i+1}^{j+1} + 6u_i^{j+1} - 4u_{i-1}^{j+1} + u_{i-2}^{j+1} \right) \\ + \left(u_{i+2}^{j} - 4u_{i+1}^{j} + 6u_i^{j} - 4u_{i-1}^{j} + u_{i-2}^{j} \right) \end{matrix} \right) \\ + \frac{1}{2} \left(Gr\left(\Theta_i^{j+1} + \Theta_i^{j} \right) + Gm\left(\Phi_i^{j+1} + \Phi_i^{j} \right) \right) \end{matrix} \right\}, \end{aligned} \tag{21}$$

$$\frac{\Pi(\alpha)}{2\alpha}\left\{\begin{array}{l}\frac{\Theta_i^{j+1}-\Theta_i^j}{\lambda}\\ +\sum_{j=1}^{m}\left(\frac{\Theta_i^{j+1-m}-\Theta_i^{j-m}}{\lambda}\right)\end{array}\right\}\varpi_{j,m}$$
$$=\beta t^{\beta-1}\left\{\begin{array}{l}\frac{1}{h_2}\left\{\frac{1}{2h^2}\left(\begin{array}{l}\left(\Theta_{i+1}^{j+1}-2\Theta_i^{j+1}+\Theta_{i-1}^{j+1}\right)\\ +\left(\Theta_{i+1}^{j}-2\Theta_i^{j}+\Theta_{i-1}^{j}\right)\end{array}\right)\right\}\\ +\psi\left(\frac{1}{4h}\left(\begin{array}{l}\left(\Theta_{i+1}^{j+1}+\Theta_{i-1}^{j+1}\right)\\ +\left(\Theta_{i+1}^{j}+\Theta_{i-1}^{j}\right)\end{array}\right)\right)^2\end{array}\right\}, \quad (22)$$

$$\frac{\Pi(\alpha)}{2\alpha}\left\{\frac{\Phi_i^{j+1}-\Phi_i^j}{\lambda}+\sum_{j=1}^{m}\left(\frac{\Phi_i^{j+1-m}-\Phi_i^{j-m}}{\lambda}\right)\right\}\varpi_{j,m}$$
$$=\beta t^{\beta-1}\left\{\Im\frac{1}{2h^2}\left(\begin{array}{l}\left(\Phi_{i+1}^{j+1}-2\Phi_i^{j+1}+\Phi_{i-1}^{j+1}\right)\\ +\left(\Phi_{i+1}^{j}-2\Phi_i^{j}+\Phi_{i-1}^{j}\right)\end{array}\right)\right\}, \quad (23)$$

consider that $y_i = ih, 0 \leqslant i \leqslant M$ with $Mh = 1$ and $t_j = j\text{ƛ}, 0 \leqslant n \leqslant N$.

3. Nusselt and Sherwood number

The Nusselt and Sherwood numbers are expressed in unitless form as follows (Ali et al., 2020):

$$Nu = -\frac{k_{nf}}{k_{TO}}\frac{\partial\Theta}{\partial\zeta}\Big|_{\zeta=0}, \quad (24)$$

$$S_h = -D_{nf}\left(\frac{\partial\Phi}{\partial\zeta}\right)_{\zeta=0}. \quad (25)$$

4. Results and discussion

Non-linear couple stress nanofluid model has been evaluated in a microchannel. The ordinary mathematical model has been converted into a fractal-fractional model by using the operator of CF and fractal dimension. The non-dimensional form of the generalized governing equations has been discretized. The numerical solution has been obtained through the Crank-Nicolson technique. Graphs for the embedded parameters have been drawn to provide an insight into the phenomenon.

To see the comparative features of fractal-fractional, fractal, fractional and classical order models, Fig. 2. has been plotted from the obtained numerical solution. From the figure, it can be seen that one can easily sketch the graph for fractal dimension, fractional and classical order from the fractal-fractional solution by adjusting their generalized parameters. There is a stronger memory effect observed in fractal-fractional order operators as a result of the additional fractal dimensions involved, as compared to simple fractional and classical order operators. There is a stronger memory effect associated with fractal-fractional models, making them more realistic and practical. Additionally, experimentalists are able to compare the results of their work in more than one fluid layer by simply adjusting the fractal-fractional parameter.

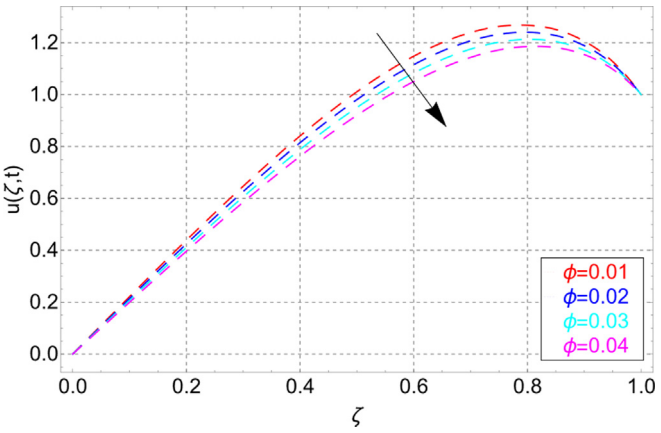

Fig. 3a. Velocity field in response to ϕ.

A dispersion of nanoparticles within a fluid is depicted in Fig. 3a by showing the resulting change in velocity field caused by their dispersal. The addition of nanoparticles to a fluid can decrease the velocity profile due to increased viscosity, which leads to increased resistance to flow. This increased resistance can result in a decreased velocity of the fluid as it moves through a channel or pipe, causing the velocity profile to flatten. So as the cadmium telluride concentration increases, the viscous layer becomes stronger, reducing fluid mobility within the microchannel. Additionally, the size and concentration of nanoparticles in the fluid can also play a role in the extent to which they affect the velocity profile. This finding suggests that using cadmium telluride particles in transformer oil can improve its lubricating properties significantly. The upshots of external pressure G on the motion of the fluid have been drawn in Fig. 3b. Fig. 3b shows acceleration in the fluid motion for higher magnitude of G. As the value of G increases the normal stresses on the fluid surface increase and due to this effect the fluid motion accelerates.

To analyze the behavior of fluid in response to Gr, Fig. 4a has been plotted. In the figure, we can clearly see that an increasing

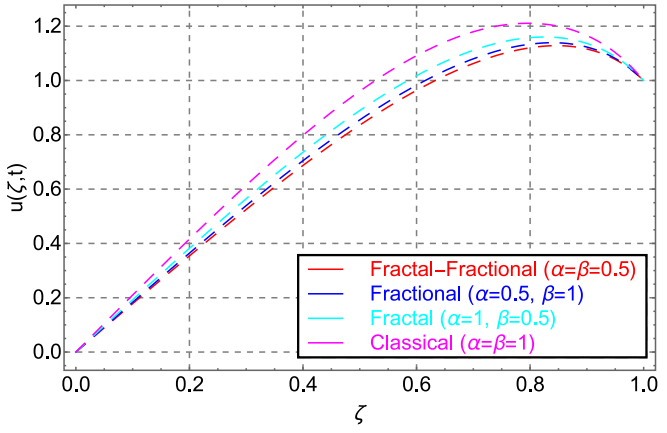

Fig. 2. Velocity fields of clclassical, fractals, fractions, and fractals-fractional order models.

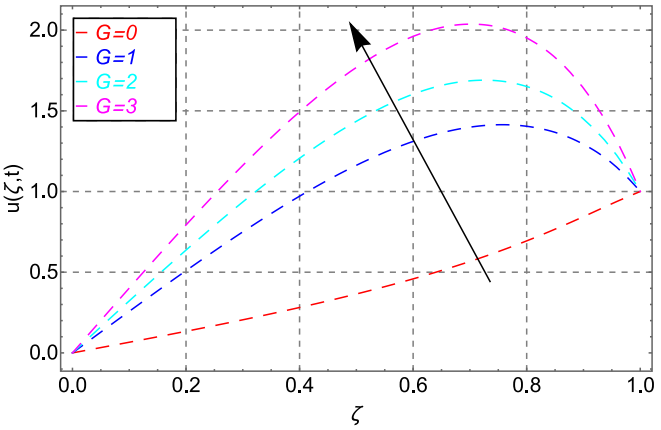

Fig. 3b. Velocity field in response to G.

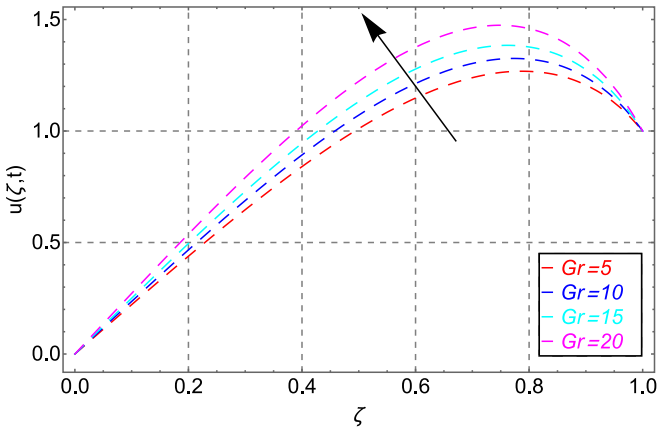

Fig. 4a. Velocity field in response to *Gr*.

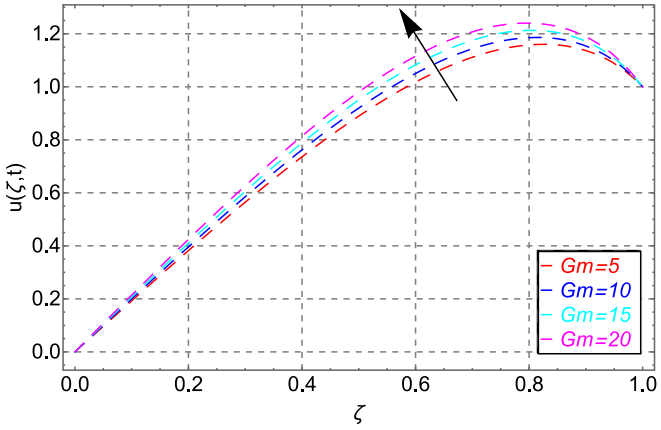

Fig. 4b. Velocity field in response to *Gm*.

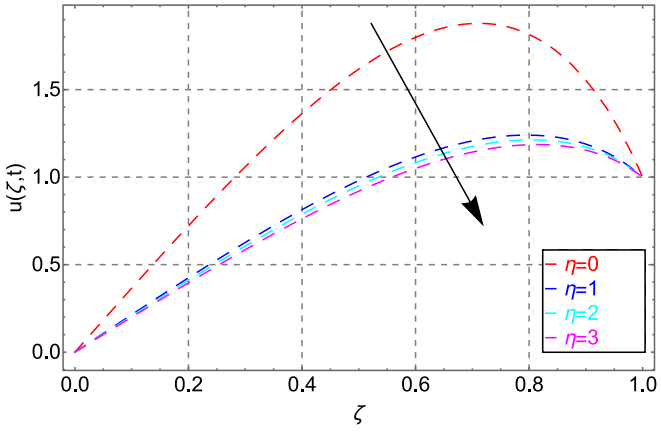

Fig. 5a. Velocity field in response to η.

value of Gr accelerates fluid motion. It is due to buoyancy forces that occur in the fluid due to the higher temperature, and therefore the fluid is accelerated due to the buoyancy forces. Fig. 4b illustrates that similar results are observed for larger values of the mass Grashof number *Gm*. This tendency can be explained by the fact that increasing the magnitude of *Gm* causes the concentration level in the fluid to rise. This causes the fluid to move faster as a result.

It can be seen in Fig. 5a how the couple stress parameter η affects the distribution of velocity as a result of the couple stress parameter. When the couple stress parameter is increased, the

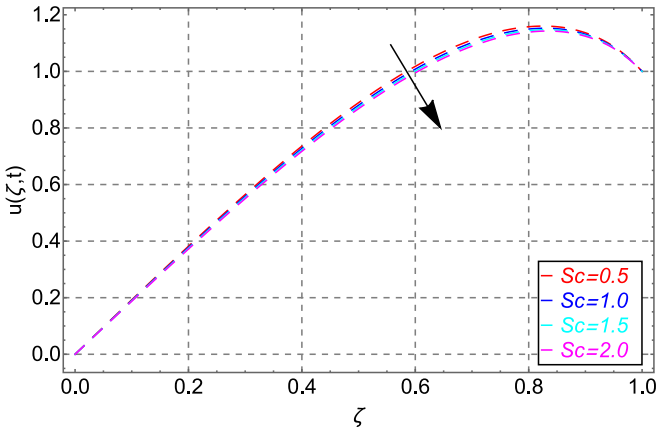

Fig. 5b. Velocity field in response to *Sc*.

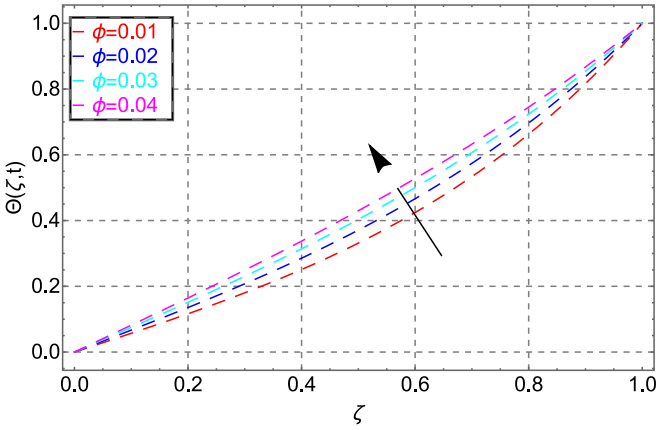

Fig. 6a. . Temperature field in response to ϕ.

nanofluid's velocity drops. Because of the nanoparticles dispersed in transformer oil, this variation occurs. Certain additives scatter in a fluid by opposing the forces they create. As fluids move, a couple of forces and stresses are created as a result of opposing forces. Due to these opposing forces, fluid motion is slows down. In order to see the behavior of velocity field of the base fluid against Schmidth number *Sc*, Fig. 5b has been portrayed through Mathematica. From sketch decreasing patteren of the velocity profile can be noticed for larger values of *Sc*. It is because of a rise in the viscous forces of fluid that this trend in the velocity profile exists.

Fig. 6a illustrates the changes in the thermal energy distribution caused by cadmium telluride concentration in transformer oil based on changes in the volume fraction of the metal. The temperature profile of transformer oil is influenced by many factors, including the material properties of the insulation, the load on the transformer, and the ambient temperature. The presence of cadmium telluride nanoparticles in the transformer oil may potentially increase the temperature profile, but the effect would depend on the specifics of the system. In general, nanoparticles can enhance heat transfer in a fluid by increasing the convective heat transfer due to their high surface area to volume ratio. If the cadmium telluride nanoparticles are dispersed in the transformer oil, they may increase the overall heat transfer rate in the fluid, leading to an increase in the temperature profile. It is important to note that the effect of nanoparticles on the temperature profile would also depend on the size and concentration of the particles, as well as the viscosity of the oil and other system parameters. Further

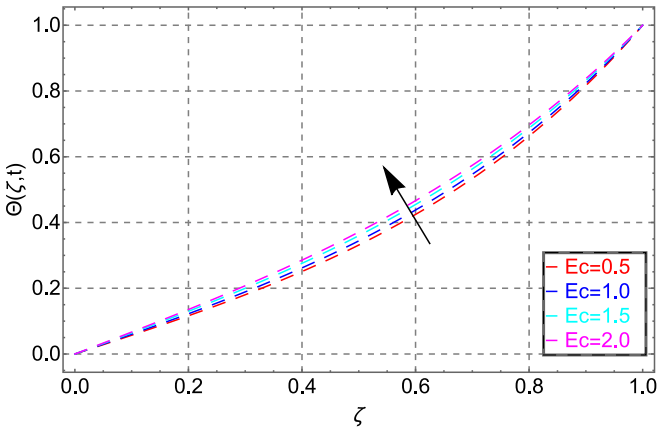

Fig 6b. Temperature field in response to *Ec.*

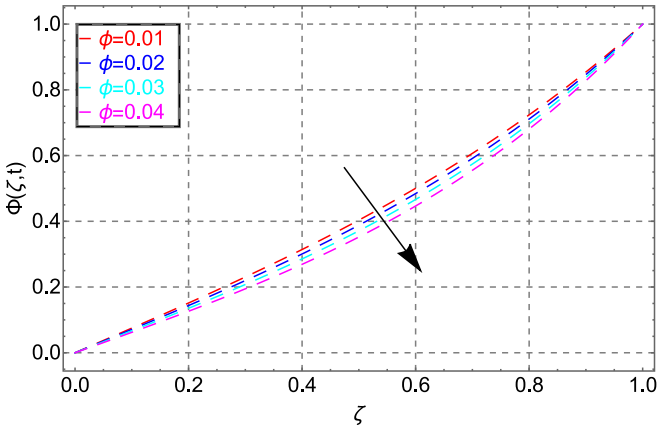

Fig. 7a. Concentration field in response to ϕ.

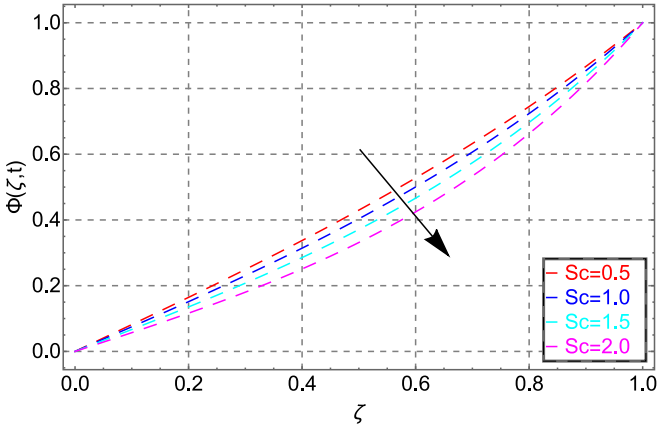

Fig. 7b. Concentration field in response to *Sc.*

research would be needed to determine the specific impact of cadmium telluride nanoparticles on the temperature profile of transformer oil. Fig. 6b shows how the Eckert number affects the transfer of heat. When the Eckert number is increased, the temperature profile tends to rise with an increasing magnitude, as shown in the graph. Eckert numbers are dimensionless numbers that describe the transfer of heat from one fluid to another in fluid mechanics. It is defined as the ratio of convective heat transfer to conductive heat transfer. A higher Eckert number indicates an increase in convective heat transfer compared to conductive heat transfer, which results in a higher temperature profile of the fluid. The reason behind this is that convective heat transfer increases the rate of heat transfer throughout the fluid, which can lead to a more uniform temperature distribution throughout the fluid.

Variation in concteration in response to volume fraction of nanoparticle are portrayed in Fig. 7a. Cadmium telluride nanoparticles increase the concentration profile of transformer oil when they are introduced into the fluid, but the effect would depend on various factors such as the size and distribution of the nanoparticles, the viscosity of the oil, and the conditions in the transformer. In general, nanoparticles can increase the concentration profile of a fluid if they are not evenly dispersed and tend to concentrate in certain regions of the fluid due to differences in fluid flow, buoyancy, or other factors. This can lead to variations in the properties of the fluid and potentially impact the performance of the transformer. It is important to note that while nanoparticles can potentially increase the concentration profile of transformer oil, they may also have other effects on the properties and performance of the oil, and these would need to be carefully evaluated. The impact of nanoparticles on the concentration profile would likely depend on the specifics of the system and would require further research to determine. The upshots of *Sc* on conetration profile are plotted in Fig. 7b. The figure shows decreasing trend in its profile in response to the higher values of *Sc*. This change in the profile is due to the inverse relationship of mass diffusion reate and Sc. So as the value of Sc gets up the diffusion rate gets slow and as a result the profile of concetration slow decreasing trend.

Table 2 shows the response to dispersion of nano particles in mineral transformer oil in terms of heat and mass transfer. Interestingly, Sherwood's and Nusselt's numbers have shown opposite trends in terms of variation. In MTO, when the volume fraction reaches 0.04, the heat transfer rate has increased, but the mass transfer rate has decreased. As a result the rate of heat transfer is increased by 15.27%. the mass transfer rate decreased by 2.07%.

5. Concluding remarks

We have investigated the non-linear fractal-fractional model of couple stress nanofluid using a numerical approach, which is based on fractal-fractional theory. Viscose dissipation was considered during the investigation. Firstly, the classical model has been formulated with help of constitutive equations and then generalized via the operator of fractal-fractional detivative. After generalization the model has been non-dimensiolized with the help of non-dimensionless entities. The numerical solution to the non-dimesnionless model has been obtained via Crank-Nicolson

Table 2
Nusselt and Sherwood number for MTO based-Cadmium Telluride.

ϕ	*Nu*	Heat Transfer Enhancement	S_h	Decrease in Mass Distribution
0	2.763	–	3.287	–
1%	2.895	3.47%	3.268	0.58%
2%	2.982	7.93%	3.252	1.06%
3%	3.086	11.69%	3.237	1.52%
4%	3.185	15.27%	3.219	2.07%

scheme. For graphical study the computational software mathematica has been used. The key points from the present analysis are addressed below:

- It is observed that for larger of Gr, Gm and G, velocity increases while retards with small values of ϕ Sc and η.
- The thermal boundary layer shows a increasing behavior against ϕ, Ec and t.
- Concentration field upsurges against Sc and ϕ.
- Increasing cadmium telluride nanoparticle volume fraction to 0.04 significantly increases heat transfer rate of the system, which reaches a significant increase of 15.27% after adding 4% cadmium telluride nanoparticles.
- The mass transfer rate increases significantly up to 2.07% when the fraction of cadmium telluride nanoparticles reaches 0.04, indicating that it improves the process of mass transfer when the amount of nanoparticles reaches 0.04.

Funding

National Natural Science Foundation of China (No. 71601072), the Fundamental Research Funds for the Universities of Henan Province (No. NSFRF210314) and Innovative Research Team of Henan Polytechnic University (No. T2022-7).

Declaration of Competing Interest

The authors declare that they have no known competing financial interests or personal relationships that could have appeared to influence the work reported in this paper.

Acknowledgment

The authors are thankful to the King Saud University for the support through Researchers Supporting Project number (RSP2023R401), King Saud University, Riyadh, Saudi Arabia.

Appendix A. Supplementary material

Supplementary data to this article can be found online at https://doi.org/10.1016/j.jksus.2023.102618.

References

Abro, K.A., Atangana, A., 2020. A comparative study of convective fluid motion in rotating cavity via Atangana-Baleanu and Caputo-Fabrizio fractal–fractional differentiations. Eur. Phys. J. Plus 135 (2), 1–16. https://doi.org/10.1140/EPJP/S13360-020-00136-X.

Ahmad, Z., Ali, F., Khan, N., Khan, I., 2021. Dynamics of fractal-fractional model of a new chaotic system of integrated circuit with Mittag-Leffler kernel. Chaos, Solitons & Fractals 153,. https://doi.org/10.1016/J.CHAOS.2021.111602 111602.

Akhtar, S., Shah, N.A., 2018. Exact solutions for some unsteady flows of a couple stress fluid between parallel plates. Ain Shams Eng. J. 9, 985–992. https://doi.org/10.1016/J.ASEJ.2016.05.008.

Ali, F., Ahmad, Z., Arif, M., Khan, I., Nisar, K.S., 2020. A time fractional model of generalized couette flow of couple stress nanofluid with heat and mass transfer: applications in engine oil. IEEE Access 8, 146944–146966. https://doi.org/10.1109/ACCESS.2020.3013701.

Almalahi, M.A., Abdo, M.S., Panchal, S.K., 2021a. Existence and Ulam-Hyers stability results of a coupled system of ψ-Hilfer sequential fractional differential equations. Results Appl. Math. 10,. https://doi.org/10.1016/J.RINAM.2021.100142 100142.

Almalahi, M.A., Panchal, S.K., Jarad, F., 2021b. Stability results of positive solutions for a system of ψ -Hilfer fractional differential equations. Chaos, Solitons & Fractals 147, 110931. https://doi.org/10.1016/J.CHAOS.2021.110931.

Almalahi, M.A., Panchal, S.K., Jarad, F., Abdeljawad, T., 2021c. Ulam–Hyers–Mittag-Leffler stability for tripled system of weighted fractional operator with TIME delay. Adv. Differ. Equations 2021, 1–18. https://doi.org/10.1186/S13662-021-03455-0/METRICS.

Arif, M., Ali, F., Sheikh, N.A., Khan, I., 2019. Enhanced heat transfer in working fluids using nanoparticles with ramped wall temperature: applications in engine oil. Res. Artic. Adv. Mech. Eng. 11, 1–11. https://doi.org/10.1177/1687814019880987.

Atangana, A., 2017. Fractal-fractional differentiation and integration: Connecting fractal calculus and fractional calculus to predict complex system. Chaos, Solitons & Fractals 102, 396–406. https://doi.org/10.1016/J.CHAOS.2017.04.027.

Atangana, A., İğret Araz, S., 2020. New numerical approximation for Chua attractor with fractional and fractal-fractional operators. Alexandria Eng. J. 59, 3275–3296. https://doi.org/10.1016/J.AEJ.2020.01.004.

Atangana, A., Qureshi, S., 2019. Modeling attractors of chaotic dynamical systems with fractal–fractional operators. Chaos, Solitons & Fractals 123, 320–337. https://doi.org/10.1016/J.CHAOS.2019.04.020.

Biomechanics, L.S.-J. of, 1985, undefined, n.d. Flow of couple stress fluid through stenotic blood vessels. Elsevier.

Choi, S., Eastman, J., 1995. Enhancing thermal conductivity of fluids with nanoparticles.

Ellahi, R., Zeeshan, A., Hussain, F., Symmetry, A.A.-, 2019, undefined, n.d. Peristaltic blood flow of couple stress fluid suspended with nanoparticles under the influence of chemical reaction and activation energy. mdpi.com.

Ghaffarkhah, A., Afrand, M., Talebkeikhah, M., Sehat, A.A., Moraveji, M.K., Talebkeikhah, F., Arjmand, M., 2020. On evaluation of thermophysical properties of transformer oil-based nanofluids: a comprehensive modeling and experimental study. J. Mol. Liq. 300,. https://doi.org/10.1016/J.MOLLIQ.2019.112249 112249.

Hamilton, R.L., Crosser, O.K., 1962. Thermal conductivity of heterogeneous two-component systems. I&EC Fundam. 1, 182–187.

Hasin, F., Ahmad, Z., Ali, F., Khan, N., Khan, I., 2022. A time fractional model of Brinkman-type nanofluid with ramped wall temperature and concentration 168781322210960 Adv. Mech. Eng. 14. https://doi.org/10.1177/16878132221096012.

Heydari, M.H., 2020. Numerical solution of nonlinear 2D optimal control problems generated by Atangana-Riemann-Liouville fractal-fractional derivative. Appl. Numer. Math. 150, 507–518. https://doi.org/10.1016/J.APNUM.2019.10.020.

Hussain, F., Ellahi, R., Zeeshan, A., Liquids, K.V.-J. of M., 2018, undefined, n.d. Modelling study on heated couple stress fluid peristaltically conveying gold nanoparticles through coaxial tubes: a remedy for gland tumors and arthritis. Elsevier.

International, J.L.-T., 1998, undefined, n.d. Squeeze film characteristics of finite journal bearings: couple stress fluid model. Elsevier.

Khan, M.I., Puneeth, V., 2021. Isothermal autocatalysis of homogeneous–heterogeneous chemical reaction in the nanofluid flowing in a diverging channel in the presence of bioconvection. https://doi.org/10.1080/17455030.2021.2008547.

Masuda, H., Ebata, A., Teramae, K., 1993. Alteration of thermal conductivity and viscosity of liquid by dispersing ultra-fine particles. Dispersion of Al_2O_3, SiO_2 and TiO_2 ultra-fine particles.

Maxwell James C., 1873. A Treatise on Electricity and Magnetism. Vol. 116, pp. 702–709. https://doi.org/10.1541/IEEJIAS.116.702.

Murtaza, S., Iftekhar, M., Ali, F., Aamina, K., Khan, I., 2020. Exact analysis of non-linear electro-osmotic flow of generalized maxwell nanofluid: applications in concrete based nano-materials. IEEE Access 8, 96738–96747. https://doi.org/10.1109/ACCESS.2020.2988259.

Murtaza, S., Kumam, P., Ahmad, Z., Sittithakerngkiet, K., Ali, I., 2022a. Finite difference simulation of fractal-fractional model of electro-osmotic flow of casson fluid in a micro channel. IEEE Access, 1. https://doi.org/10.1109/ACCESS.2022.3148970.

Murtaza, S., Kumam, P., Kaewkhao, A., Khan, N., Ahmad, Z., 2022b. Fractal fractional analysis of non linear electro osmotic flow with cadmium telluride nanoparticles. Sci. Rep. 12 (1), 1–16. https://doi.org/10.1038/s41598-022-23182-0.

Naduvinamani, N.B., Kashinath, B., 2006. Surface roughness effects on curved pivoted slider bearings with couple stress fluid. Lubr. Sci. 18, 293–307. https://doi.org/10.1002/ls.24.

Pralhad, R.N., Schultz, D.H., 2004. Modeling of arterial stenosis and its applications to blood diseases. Math. Biosci. 190, 203–220. https://doi.org/10.1016/J.MBS.2004.01.009.

Ramesh, K., Engineering, M.D.-N., 2019, undefined, n.d. Effect of endoscope on the peristaltic transport of a couple stress fluid with heat transfer: Application to biomedicine. degruyter.com.

Rasheed, H.U., Islam, S., Helmi, M.M., Alsallami, S.A.M., Khan, Z., Khan, I., 2021. An analytical study of internal heating and chemical reaction effects on MHD flow of nanofluid with convective conditions. Crystals 11, 1523. https://doi.org/10.3390/CRYST11121523.

Shahzad, F., Baleanu, D., Jamshed, W., Nisar, K.S., Eid, M.R., Safdar, R., Ismail, K.A., 2021. Flow and heat transport phenomenon for dynamics of Jeffrey nanofluid past stretchable sheet subject to Lorentz force and dissipation effects. Sci. Rep. 11 (1), 1–15. https://doi.org/10.1038/s41598-021-02212-3.

Shit, G., Liquids, N.R.-J. of M., 2016, undefined, n.d. Role of slip velocity on peristaltic transport of couple stress fluid through an asymmetric non-uniform channel: application to digestive system. Elsevier.

Stokes, V.K., Stokes, V.K., 1984. Couple Stresses in Fluids. In: Theories of Fluids with Microstructure. Springer, Berlin Heidelberg, pp. 34–80. https://doi.org/10.1007/978-3-642-82351-0_4.

Tripathi, D., 2011. Peristaltic flow of couple-stress conducting fluids through a porous channel: applications to blood flow in the micro-circulatory system. J. Biol. Syst. 19, 461–477. https://doi.org/10.1142/S021833901100407X.